Intensity fluctuation spectrum of the nonlinear resonance fluorescence of an atomic system

D. F. Smirnov and A. S. Troshin

Leningrad State Pedagogic Institute
(Submitted November 30, 1976)
Zh. Eksp. Teor. Fiz. 72, 2055–2063 (June 1977)

The intensity fluctuation spectrum (as defined by the fourth order field correlator) of the resonance fluorescence of an atomic system under stationary excitation by intense monochromatic light is investigated. The spectrum contains components due to scattering from individual atoms and from groups of two, three, and four atoms. Interference effects lead to a dependence of the observed spectrum on the shape of the photodetector. Variants of the experiment are discussed, which enable one to isolate different components of the spectrum; taken together, these components carry information on the strong-field behavior of the atomic density matrix.

PACS numbers: 32.50.+d

1. INTRODUCTION

The intensity fluctuation spectrum of radiation may carry information in addition to that carried by the ordinary optical spectrum. The intensity fluctuation spectrum of the spontaneous emission from a system of atoms under broad band pumping has been investigated by Aleksandrov et al.[1,2] In this case the fluctuation spectrum is the sum of the beat spectrum of the spontaneous emission components and the converted pumping intensity fluctuation spectrum. A component of width equal to the radiative width of the excited level could be distinguished in the spectrum despite the predominant Doppler broadening.

Here we consider the intensity fluctuations of the stationary resonance scattering of laser light by a system of identical atoms. The two-level approximation will be used for the scattering atom, and the exciting light will be assumed to be monochromatic and linearly polarized. The nonlinear resonance scattering of monochromatic light by a two-level system has previously been investigated by Mollow[3] and by us[4]. This process includes coherent scattering and nonlinear incoherent scattering; in a strong enough field (see below) the scattering (or resonance fluorescence) spectrum consists of three broadened lines. The fluctuation spectrum found in the present work, which is determined by the fourth order field correlator (formula (1)), contains contributions from the secondary radiation emitted by individual atoms (the single-atom effect) and by groups of two, three, and four atoms (several-atom effects). The characteristic angular dependence associated with interference incident to scattering of light from groups of atoms leads to selectivity with respect to different regions of the photodetector surface. When a single photodetector is used, one can distinguish one part or another of the fluctuation spectrum, depending on the shape of the detector. By using two photodetectors one can observe the single-atom effect. The latter arises only in the nonlinear problem and makes it possible to observe the population modulation of the excited atomic level due to the resonant action of the strong field.

The diagram technique of time-dependent perturbation theory is used for the density matrix.[5,6] This technique has been used, in particular, to investigate both nonlinear scattering[4] and the fluctuation spectrum of spontaneous emission.[7]

2. RELATION BETWEEN THE PHOTOCURRENT CORRELATOR AND THE DENSITY MATRIX OF THE ATOMIC SYSTEM

In the experimental study of intensity fluctuations one measures the spectrum of the second order stationary photocurrent correlator $K(t_1, t_2) = (\frac{1}{2})\langle [J(t_1), J(t_2)]_+\rangle$. According to Glauber's photodetector model[8] this quantity can be expressed as a sum of averages of field-operator products[7]:

$$K(t_1, t_2) = \frac{e^2 q}{2\pi\omega_0}\delta(t_2 - t_1)\sum_{\alpha = x, y, z}\int ds\langle E_\alpha^{(-)}(\mathbf{r}, t_2)E_\alpha^{(+)}(\mathbf{r}, t_1)\rangle$$

$$+ \left(\frac{eq}{2\pi\omega_0}\right)^2\sum_{\alpha, \beta = x, y, z}\int ds_1\int ds_2[\langle E_\alpha^{(-)}(\mathbf{r}_1, t_1)E_\beta^{(-)}(\mathbf{r}_2, t_2)$$

$$\times E_\beta^{(+)}(\mathbf{r}_2, t_2)E_\alpha^{(+)}(\mathbf{r}_1, t_1)\rangle\theta(t_2 - t_1) + \langle E_\alpha^{(-)}(\mathbf{r}_2, t_2)E_\beta^{(-)}(\mathbf{r}_1, t_1)$$

$$\times E_\beta^{(+)}(\mathbf{r}_1, t_1)E_\alpha^{(+)}(\mathbf{r}_2, t_2)\rangle\theta(t_1 - t_2)]. \qquad (1)$$

Here e is the electron charge, q is the photodetector quantum yield, ω_0 is the frequency of the exciting light, $\theta(\tau)$ is the unit step function ($\theta(\tau) = 1$ when $\tau > 0$ and $\theta(\tau) = 0$ when $\tau < 0$), and the integration is taken over the photodetector surface. The first term in Eq. (1) represents the shot noise, and the second term represents the information-bearing part of the photocurrent correlator. The quantity (1), which characterizes the scattered radiation, is determined by the behavior of the scattering atoms in the strong field of the incident light wave. The time dependences of the Heisenberg operators $E_\alpha^{(\pm)}(r, t)$ in Eq. (1) are determined by the Hamiltonian operator $H = H_0 + H_I + V(t)$. Here H_0 is the Hamiltonian operator for the system of N two-level atoms (transition frequency ω_{21}) and the free quantized electromagnetic field; H_I represents the interaction between the atoms and the field, and is given by

$$H_I = -\sum_{a=1}^{N} \mathbf{d}_a \mathbf{E}(\mathbf{r}_a), \qquad (2)$$

where $\mathbf{d}_a$ is the dipole moment operator for atom a,

$$E(r) = E^{(+)}(r) + E^{(-)}(r),$$

$$E^{(\pm)}(r) = \pm i \sum_{k,\mu} \left(\frac{2\pi\omega_{k,\mu}}{L^3} \right)^{1/2} e_\mu c_{k,\mu}^{(\mp)} e^{ikr} \qquad (3)$$

$(\hbar = c = 1)$; and $V(t)$ represents the interaction of the atoms with the classical field of the incident light wave:

$$V(t) = -\frac{1}{2} \sum_{a=1}^{n} d_a E_0 \exp\{-i\omega_0 t + ik_0 r_a\} + \text{c.c.} \qquad (4)$$

Let us consider the integrand in the second term of Eq. (1) for $t_2 > t_1$:

$$\sum_{\alpha,\beta=x,y,z} \langle E_\alpha^{(-)}(r_1, t_1) E_\beta^{(-)}(r_2, t_2) E_\beta^{(+)}(r_2, t_2) E_\alpha^{(+)}(r_1, t_1) \rangle$$

$$= \sum_{\alpha,\beta=x,y,z} \text{Sp} \{ E_\beta^{(+)}(r_2) S(t_2, t_1) E_\alpha^{(+)}(r_1) S(t_1) \rho_0 S^+(t_1)$$

$$\times E_\alpha^{(-)}(r_1) S^+(t_2, t_1) E_\beta^{(-)}(r_2) \}. \qquad (5)$$

Here $S(t_2, t_1)$ is the unitary operator specifying the time evolution of the system, and ρ_0 is the density matrix of the system at the initial time and corresponds to the ground states of the atoms and the quantized electromagnetic field. The quantity (5), and accordingly the operator $S(t_2, t_1)$, must be calculated accurately as regards $V(t)$ (in the resonance approximation) and H_I (treating the quantized electromagnetic field as a thermostat at zero temperature). We shall use a diagram method. A typical diagram representing expression (5) has the form

$$(6)$$
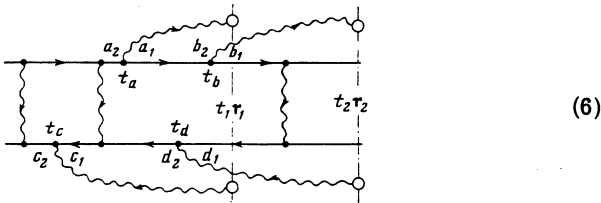
Traversing the contour of the diagram along the horizontal lines in the direction of the arrows from time t_2 on the lower line corresponds to reading expression (5) from the right to the left. The large open circles on the vertical sections at t_1 and t_2 represent the operators $E_\alpha^{(\pm)}(r_i)$, and the small black circles, the interaction H_I (successive integrations over the times of all the vertices are to be made). Each horizontal line describes the development of the amplitude for the state of the system of N atoms. The interactions between the atoms are neglected, but the radiative broadening and the action of the field of the incident light wave are taken accurately into account in the line for an individual atom.[4] The diagrams are taken in the zeroth approximation in the parameter γ/ω_{21}, where γ is the radiative width of the excited level. We do not consider collective effects in the emission, so (in the γ/ω approximation) each vertical photon line joins vertices corresponding to transitions of one and the same atom. The atomic indices $(a_2, a_1, b_2, b_1, \ldots)$ denote only transitions in which detected photons are emitted (a_1 represents the

ground state and a_2 the excited state of atom a). A summation over the states of the other atoms is to be taken in each of the diagrams (6), and then the diagrams are to be summed over all sets of atomic indices (a, b, c, d). Thus, the fourth order field correlator is determined by the secondary emission from individual atoms and from groups of two, three, and four atoms.

For a photon line in diagram (6), corresponding, for example, to the emission of a photon at time t_a by atom a and its absorption at time t_1 by an atom at point r_1 on the photodetector surface, we can obtain the following expression (valid within the wave zone):

$$\varepsilon(r_{a,1}, t_a, t_1) = \frac{\omega_0^2}{r_{a,1}} [d - n_{a,1}(dn_{a,1})] \delta(t_1 - t_a - r_{a,1}) \exp\{-i\omega_0(t_1 - r_{a,1})\}. \qquad (7)$$

Here $r_{a,1} = r_1 - r_a$ and $n_{a,1} = r_{a,1}/r_{a,1}$; the condition $\gamma/\omega_{21} \ll 1$ has been used in summing over the photon wave vector and polarization; and the factors $\exp\{\pm i\omega_0 t\}$ and $\exp\{\pm i\omega_{21} t\}$ have been regrouped for convenience in what follows.

Let us suppose that the geometry of the experiment is such that the difference between the light propagation times from the scattering atoms to different points on the photodetector surface are small as compared with the characteristic times of the systems. Then retardation will have no effect on the spectrum of the correlator that we are interested in. We shall therefore ignore retardation entirely, introducing the supplementary conditions

$$L \ll R \ll \min\{\gamma^{-1}, |v_0|^{-1}, V_0^{-1}\}, \qquad (8)$$

in which L is a characteristic linear dimension of the system (the scattering region), R is the distance to the photodetector, $v_0 = \omega_0 - \omega_{21}$ is the deviation from resonance, and $V_0 = (\frac{1}{2})|d \cdot E_0|$, where d is the transition dipole moment. Under this assumption, the four photon lines in diagram (6) that represent detected photons become vertical ($t_a = t_c = t_1$ and $t_b = t_d = t_2$).

Summation of all the diagrams (6) with allowance for the approximations mentioned above corresponds to replacing the fragment of the diagram up to time t_1 and the fragment from t_1 to t_2 by the corresponding elements of the N-atom density matrix, calculated accurately as regards H_I and $V(t)$. The N-atom density matrix is a direct (outer) product of single-atom density matrices, and the single-atom density matrix elements are calculated from the equations[4]

$$\dot{\rho}_{22} = -\gamma\rho_{22} + i[V_{12}^*\rho_{21} - V_{21}\rho_{12}],$$
$$\dot{\rho}_{12} = -(\gamma/2 + iv_0)\rho_{12} - iV_{12}^*[\rho_{22} - \rho_{11}],$$
$$\rho_{11} + \rho_{22} = 1, \qquad \rho_{21} = \rho_{12}^*. \qquad (9)$$

Here $V_{21} = V_0 \exp\{i\omega_0 n_0 \cdot r\}$. Equations (9) were derived under the same assumptions as were used in drawing diagrams (6).

3. THE SINGLE-ATOM EFFECT

The total contribution to the fourth order correlator due to scattering from individual atoms (the case $a = b = c = d$ in diagrams (6)) is

1080   Sov. Phys. JETP 45 (6), June 1977

D. F. Smirnov and A. S. Troshin   1080

$$K_1(\tau) = N(eq\gamma)^2\alpha^2\bar{p}_{22}[\rho_{22}^{(11)}(\tau)\theta(\tau) + \rho_{22}^{(11)}(-\tau)\theta(-\tau)]. \qquad (10)$$

Here and below we contemplate passing to the limit t_1, $t_2 \to \infty$ with $\tau = t_2 - t_1$ held fixed. In Eq. (10), $\bar{p}_{22}$ is the stationary value, the upper indices on $\rho_{22}^{(11)}(\tau)$ indicate the initial condition (for $\tau = 0$), and the coefficient α depends on the photodetector geometry:

$$\alpha = \int d\Omega F(\mathbf{n}), \quad F(\mathbf{n}) = \frac{3}{8\pi d^2}[d - \mathbf{n}(d\mathbf{n})]^2, \qquad (11)$$

where $\mathbf{n}$ is a unit vector directed from the scattering region toward a point on the photodetector.

Expression (10) represents the correlation of photons emitted in successive scatterings by the same atom. Since $\rho_{22}^{(11)}(\tau)$ vanishes at $\tau = 0$ and tends toward $\bar{p}_{22}$ as $\tau \to \infty$, this correlation is of antibunching type, i.e., the probability for the emission of a second photon following the first one in times of the order of $\min\{\gamma^{-1}, |\nu_0|^{-1}, V_0^{-1}\}$ is reduced.

At this point it is appropriate to point out that study of stationary scattering intensity correlations can shed light on the nonstationary behavior of an atom under given external conditions. In fact, in this case one can say that the recording of a scattered photon at time t is reliable evidence that the atom is in the ground state at that time; then the probability per unit time for recording a second photon at time $t + \tau$ will be proportional to $\rho_{22}^{(11)}(t + \tau, t)$.

To analyze the spectrum we shall use the Laplace transform of the solution to Eqs. (9):

$$\rho_{22}^{(11)}(s) = V_0^2(2s + \gamma)/D(s), \qquad (12)$$

where $D(s)$ is the determinant of Eqs. (9) and is given by

$$D(s) = s[s^3 + 2\gamma s^2 + (5\gamma^2/4 + \nu_0^2 + 4V_0^2)s + \gamma(\gamma^2/4 + \nu_0^2 + 2V_0^2)]. \qquad (13)$$

The above mentioned antibunching of photons leads to the presence of negative components in the spectrum of the $K_1(\tau)$ signal, i.e., to the presence of dips, where the spectrum falls below the shot-noise level. The shot-noise level in the spectrum is determined by the first term in Eq. (1) and, if the spectrum is observed outside the diffraction cone of the incident wave, it is given by

$$G_{sh}(\omega) = Ne^2 q\alpha\gamma\bar{p}_{22} = Ne^2 q\alpha\gamma\frac{V_0^2}{\gamma^2/4 + \nu_0^2 + 2V_0^2}. \qquad (14)$$

In the weak-field case ($V_0^2 \ll \gamma^2/4 + \nu_0^2$) the spectrum $G_1(\omega)$ of the single-atom signal has the form shown by curves a and b in Fig. 1:

$$G_1(\omega) = N(eq\gamma)^2\alpha^2\left[\frac{V_0^2}{\gamma^2/4 + \nu_0^2}\right]^2$$

$$\times 2\pi[\delta(\omega) + L_\gamma(\omega) - L_{\gamma/2}(\omega - \nu_0) - L_{\gamma/2}(\omega + \nu_0)]; \qquad (15)$$

here $L_a(x) = (a/\pi)(a^2 + x^2)^{-1}$. At $\nu_0 = 0$ and $\omega \approx 0$, for example, the signal-to-noise ratio is $24\,\alpha q(V_0^2/\gamma^2)$. When Doppler broadening is predominant ($\delta\omega_D \gg \gamma$), then un-
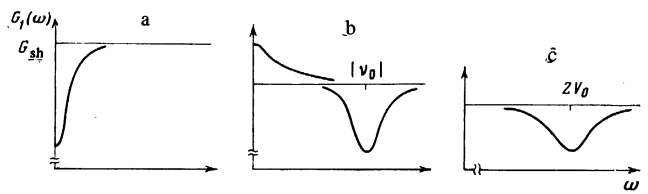

FIG. 1. Spectra of the single-atom effect in a weak field, $V_0^2 \ll \gamma^2/4 + \nu_0^2$ (a and b: a—$\nu_0 = 0$, b—$|\nu_0| = 3$) and in a strong field, $V_0^2 \gg \nu_0^2$, γ^2 (c). It is assumed that $q\alpha = 1$.

der excitation near the line center there appears a dip ($\sim L_\gamma^2(\omega)$) in the spectrum against the shot noise background, the signal-to-noise ratio in the region $\omega \approx 0$ being of that same order. It can be shown that there is a line of width of the order of γ in the spectrum at zero frequency, even when the transverse relaxation constant is large. Thus, the spectrum (15) can be used to measure γ independently of the nature of the line broadening.

In the strong field case ($V_0^2 \gg \gamma^2, \nu_0^2$), population oscillations of frequency $2V_0$ appear in the spectrum (curve c in Fig. 1):

$$G_1(\omega) = N(eq\gamma)^2\alpha^2\frac{\pi}{2}\left[\delta(\omega) - \frac{1}{2}L_{3\gamma/4}(\omega - 2V_0) - \frac{1}{2}L_{3\gamma/4}(\omega + 2V_0)\right]. \qquad (16)$$

In this case the ratio of the depth of the dip at $\omega = 2V_0$ to the shot noise level is $(\frac{2}{3})\alpha q$.

4. SEVERAL-ATOM EFFECTS

In classifying the contributions from groups of atoms we introduce an abbreviated notation for diagrams of the type of (6) summed in all orders with respect to $V(t)$ and H_I, in which only the letters designating the atoms at the four vertices are given: $(ab\,cd)$.

The diagram $(ab\,ba)$ is of interference type; on averaging over the positions of the atoms for $\lambda \ll L \ll R$ there arises the coefficient

$$\int d\Omega_1 d\Omega_2 |I(\mathbf{n}_1 - \mathbf{n}_2)|^2 F(\mathbf{n}_1)F(\mathbf{n}_2) = \beta\sigma/S, \qquad (17)$$

where

$$I(\mathbf{n}) = L^{-3}\int d\mathbf{r}\,\exp\{i\omega_0\mathbf{n}\mathbf{r}\}, \qquad (18)$$

$$\beta = \Omega\int d\Omega F^2(\mathbf{n}) \qquad (19)$$

(β is a factor of the order of unity), $\sigma \approx (\lambda^2/L^2)R^2$ is the spatial coherence area at the photodetector surface (see, e.g., Refs. 2 and 7), $S \approx R^2\Omega$, and Ω is the photon acceptance solid angle of the photodetector.

Analysis of Eq. (17) shows that the contribution from this diagram is determined by pairs of photons having roughly equal wave vectors (within the solid angle λ^2/L^2); on the whole there is no sharp directionality with respect to regions of the photocathode surface. The complete expression for the contribution of diagram $(ab\,ba)$ to the correlator has the form

$$K_2(\tau) = \beta\frac{\sigma}{S}(eq\gamma N)^2[|j(\tau)|^2\theta(\tau) + |j(-\tau)|^2\theta(-\tau)]. \qquad (20)$$

D. F. Smirnov and A. S. Troshin   1081

where the function

$$f(\tau) = \bar{p}_{21}\rho_{12}^{(11)}(\tau) + \bar{p}_{22}\rho_{12}^{(12)}(\tau) \qquad (21)$$

is related to the first order correlation function $K_1^{(I)}(\tau)$, which determines the single-atom scattering spectrum:

$$K_1^{(I)}(\tau) = \gamma[f(\tau)\theta(\tau) + f^*(-\tau)\theta(-\tau)]e^{i\omega_0\tau}. \qquad (22)$$

It follows from Eqs. (20)–(22) that

$$K_2(\tau) \sim |K_1^{(I)}(\tau)|^2.$$

Thus, the spectrum of the $K_2(\tau)$ signal is a convolution of the single-atom scattering spectrum,[4] i.e., the beat spectrum of the Fourier components of the scattered radiation ("wave noise"). In the weak field case ($V_0^2 \ll \gamma^2/4 + \nu_0^2$), when there is only coherent scattering, the $K_2(\tau)$ spectrum reduces to a line at zero frequency; in the strong field case ($V_0^2 \gg \gamma^2$, ν_0^2) it consists of broadened lines at the frequencies $\omega = 0$, $2V_0$, and $4V_0$. We note that the diagram ($ab\ ba$) corresponds to a partial factorization of the averaged fourth order field correlator:

$$\langle E_\alpha^{(-)}(1)E_\beta^{(+)}(2)\rangle\langle E_\beta^{(-)}(2)E_\alpha^{(+)}(1)\rangle.$$

In general, each diagram corresponds to a definite factorization of the correlator.

All the remaining diagrams either contribute only at zero frequency or are characterized by sharp directivity–selectivity with respect to regions of the photocathode. Here we shall consider only diagrams of the second group.

The diagram ($aa\ ab$) corresponds to the factorization

$$\langle E_\beta^{(-)}(2)\rangle\langle E_\alpha^{(-)}(1)E_\alpha^{(+)}(1)E_\beta^{(+)}(2)\rangle$$

and its contribution to the correlator is given by the expression

$$K_2'(\tau) = \alpha F(n_0)(eq\gamma N)^2 \int d\Omega |(n-n_0)|^2$$
$$\times \bar{p}_{12}\bar{p}_{22}[\rho_{(21)}^{(11)}(\tau)\theta(\tau) + \rho_{21}^{(11)}(-\tau)\theta(-\tau)]. \qquad (23)$$

Since the average value of the atomic dipole moment is proportional to $\rho_{21}(t) + $ c. c., the spectrum of expression (23) reveals nonstationary behavior of the atomic dipole moment in a strong field. An estimate of the integral in Eq. (23) is λ^2/L^2; unlike the case of Eq. (10), however, here it is directions such that $n_1 \approx n_0$ (within the diffraction angle λ^2/L^2) that are most important. If the observations are made in such a manner that $|n_1 - n_0| \approx 1$, i.e., if the central region of the photocathode (corresponding to the direction n_0) is absent, the integral in Eq. (23) will be of the order of λ^3/L^3; then the contribution from the diagram ($aa\ ab$) will be much smaller than that of the diagram ($ab\ ba$), and if $N(\lambda^3/L^3) \ll 1$, it will also be much smaller than the single-atom signal. If an experiment in which delayed coincidences are counted between photon pairs with wave vectors in directions n_1 and n_2 such that $n_1 \approx n_0$ and $|n_2 - n_0| \approx 1$ ("sideward-forward"), the quantity $K_2'(\tau)$ exceeds all the others. Analogous estimates can be obtained for the

other nontrivial two-atom diagrams.

When photon pairs are recorded in a small solid angle about the direction n_0, the three-atom diagrams are the most important ones. The diagram ($ab\ ca$) corresponds to the factorization

$$\langle E_\alpha^{(-)}(1)\rangle\langle E_\beta^{(+)}(2)\rangle\langle E_\beta^{(-)}(2)E_\alpha^{(+)}(1)\rangle$$

and to the expression

$$K_3'(\tau) = N^3(eq\gamma F(n_0))^2 \int d\Omega_1\, d\Omega_2 I^*(n_1 - n_0)I(n_2 - n_0)$$
$$\times I(n_1 - n_2)|\bar{p}_{21}|^2[f(\tau)\theta(\tau) + f(-\tau)\theta(-\tau)], \qquad (24)$$

in which $f(\tau)$ is defined by Eq. (21). An upper estimate for the integral in Eq. (24) is λ^4/L^4; when the observations are limited by the condition $|n_1 - n_0| \approx |n_2 - n_0| \approx 1$ we obtain the estimate λ^6/L^6. When $N(\lambda^3/L^3) \ll 1$ the contribution from this diagram is much smaller than both the single-atom contribution and the wave noise. The diagrams ($ab\ ca$) and ($ba\ ac$) are of interest in connection with the spectrum because here, as is evident from Eqs. (24) and (22), the single-atom scattering spectrum is reproduced, but shifted to zero frequency (because of beating with the coherent scattering component within the diffraction cone of the incident wave).

The diagrams ($aa\ bc$) and ($bc\ aa$) are responsible for correlations of another kind, which are associated with the conversion of photons according to the scheme $2k_0 = k_1 + k_2$. The diagram ($aa\ bc$) corresponds to the factorization

$$\langle E_\alpha^{(-)}(1)\rangle\langle E_\beta^{(-)}(2)\rangle\langle E_\beta^{(+)}(2)E_\alpha^{(+)}(1)\rangle$$

and to the expression

$$K_3''(\tau) = N^3(eq\gamma F(n_0))^2 \int d\Omega_1\, d\Omega_2 I(2n_0 - n_1 - n_2)I(n_1 - n_0)I(n_2 - n_0)$$
$$\times \bar{p}_{12}^2 \sum_{i=1,2} (\bar{p}_{21}\rho_{21}^{(1i)}(\tau)\theta(\tau) + \bar{p}_{21}\rho_{21}^{(1i)}(-\tau)\theta(-\tau)]. \qquad (25)$$

For the case in which photons are recorded only within the solid angle λ^2/L^2, the angular-dependence factors in Eqs. (24) and (25) are virtually the same. Here is the spectrum of the total contribution from all nontrivial three-atom diagrams for the limiting case $V_0^2 \gg \gamma^2$, ν_0^2:

$$G_3(\omega) \sim \frac{\nu_0^2}{V_0^2}L_{\gamma/2}(\omega) + \frac{\gamma^2}{2V_0^2}[L_{3\gamma/4}(\omega - 2V_0) + L_{3\gamma/4}(\omega + 2V_0)]. \qquad (26)$$

Depending on the magnitude of $\nu_0 = \omega_0 - \omega_{21}$, the deviation from resonance, one can observe either the central line or the side component in the spectrum; in particular, when $|\nu_0| \ll \gamma$, the $2k_0 = k_1 + k_2$ process favors the suppression of the central component. This conclusion is in accordance with the result obtained by Golubev,[9] who considered the beats between the incident wave and the components of the scattering spectrum.

5. CONCLUSION

Taken together, the contributions from the different groups of diagrams contain information on the behavior

D. F. Smirnov and A. S. Troshin

of the atomic density matrix in a strong field, reproduce the nonlinear fluorescence spectrum (shifted to zero frequency), and include its beat spectrum. If a single spherical photocathode is used, as was assumed above, then in the general case the entire spectrum of the correlator (1) is complex. Information of one sort or another can be extracted from experiments performed under various conditions by making use of the characteristic angular dependence—more accurately, the selectivity with respect to different regions of the photocathode. Such selectivity arises because of interference between the probability amplitudes for the processes that give rise to secondary emission from groups of atoms.

If one uses a single photocathode with its central region missing, i.e., if one detects only sideward scattered photons ($|n_{1,2} - n_0| \approx 1$), then shot noise (the constant component of the spectrum), single-atom scattering (Sec. 3), and two-atom wave noise (Sec. 4, Eq. (20)) all contribute to the spectrum. Generally speaking, the wave noise, which is proportional to $N^2\sigma/S \approx N^2\lambda^2/L^2$, is stronger than the single-atom signal (proportional to N). In a relative weak field ($V_0^2 \ll \gamma^2/4 + \nu_0^2$), however, the two signals have different field dependences (when $\omega \neq 0$), so that $G_2(\omega)/G_1(\omega) \sim N(\lambda^2/L^2)(V_0^2/\gamma^2)$. When the Doppler broadening is predominant this factor is replaced (for the region $\omega \approx 0$) by $N(\lambda^2/L^2)(V_0^2/\gamma\delta\omega_D)$. These conditions favor the observation of a line of width of the order of γ in the region $\omega \approx 0$.

Experiments using two photodetectors from which the photocurrents $J_1(t_1)$ and $J_2(t_2)$ are taken separately, like the Hanbury Brown-Twiss experiment, can be of interest. Here the expression for the correlator $\langle [J_1(t_1), J_2(t_2)]_{\downarrow} \rangle$ differs from that for $K(t_1, t_2)$ (Eq. (1)) in the absence of shot noise and in fact that the double integra-

tion in the second term in Eq. (1) is replaced by an integration over the surfaces of both photodetectors. If the two photodetectors record only photons emitted sideward in substantially different directions, the contribution to the correlator from effects due to scattering from groups of atoms will be small as compared with that from the single-atom effect. Under these conditions, therefore, one can observe the single-atom effect in isolation, either by measuring the photocurrent cross correlation spectrum, or by counting delayed coincidences between the two photon counters.

[1]E. B. Aleksandrov, V. P. Kozlov, and V. N. Klyasov, Zh. Eksp. Teor. Fiz. **66**, 1269 (1974) [Sov. Phys. JETP **39**, 620 (1974)].

[2]E. B. Aleksandrov and V. N. Kulyasov, Opt. Spektrosk., **40**, 785 (1976) [Opt. Spectrosc. (USSR) **40**, 449 (1976)].

[3]B. R. Mollow, Phys. Rev. **188**, 1969 (1969).

[4]D. F. Smirnov and A. S. Troshin, Vestnik LGU, seriya fiz. i khim. 4, 93 (1971).

[5]O. V. Konstantinov and V. I. Perel', Zh. Eksp. Teor. Fiz. **39**, 197 (1960) [Sov. Phys. JETP **12**, 142 (1961)].

[6]V. I. Perel', Author's abstract of Doctoral Dissertation, A. F. Ioffe, Phys. Tech. Inst., USSR Acad. Sci., Leningrad, 1966.

[7]D. F. Smirnov and I. V. Sokolov, Zh. Eksp. Teor. Fiz. **70**, 2098 (1976) [Sov. Phys. JETP **43**, 1095 (1976)].

[8]R. Glauber, in sb: Kvantovaya optika i kvantovaya radiofizika (Collected articles: Quantum optics and quantum radiophysics), Mir, 1966, p. 91.

[9]Yu. M. Golubev, Zh. Eksp. Teor. Fiz. **66**, 2028 (1974) [Sov. Phys. JETP **39**, 999 (1974)].

Translated by E. Brunner

1083   Sov. Phys. JETP 45 (6), June 1977

D. F. Smirnov and A. S. Troshin   1083